

RESEARCH

Open Access



# Integrating trans-omics, cellular experiments and clinical validation to identify ILF2 as a diagnostic serum biomarker and therapeutic target in gastric cancer

Shao-Song Liu<sup>1</sup>, Qin-Si Wan<sup>1</sup>, Cong Lv<sup>1</sup>, Jin-Ke Wang<sup>1</sup>, Song Jiang<sup>1</sup>, Dan Cai<sup>1</sup>, Mao-Sheng Liu<sup>1</sup>, Ting Wang<sup>1</sup> and Kun-He Zhang<sup>1\*</sup>

## Abstract

**Background** Gastric cancer (GC) lacks serum biomarkers with clinical diagnostic value. Multi-omics analysis is an important approach to discovering cancer biomarkers. This study aimed to identify and validate serum biomarkers for GC diagnosis by cross-analysis of proteomics and transcriptomics datasets.

**Methods** A cross-omics analysis was performed to identify overlapping differentially expressed genes (DEGs) between our previous aptamer-based GC serum proteomics dataset and the GC tissue RNA-Seq dataset in The Cancer Genome Atlas (TCGA) database, followed by lasso regression and random forest analysis to select key overlapping DEGs as candidate biomarkers for GC. The mRNA levels and diagnostic performance of these candidate biomarkers were analyzed in the original and independent GC datasets to select valuable candidate biomarkers. The valuable candidate biomarkers were subjected to bioinformatics analysis to select those closely associated with the biological behaviors of GC as potential biomarkers. The clinical diagnostic value of the potential biomarkers was validated using serum samples, and their expression levels and functions in GC cells were validated using in vitro cell experiments.

**Results** Four candidate biomarkers (ILF2, PGM2L1, CHD7, and JCHAIN) were selected. Their mRNA levels differed significantly between tumor and normal tissues and showed different diagnostic performances for GC, with areas under the receiver operating characteristic curve (AUROCs) of 0.629–0.950 in the TCGA dataset and 0.736–0.840 in the Gene Expression Omnibus (GEO) dataset. In the bioinformatics analysis, only ILF2 (interleukin enhancer-binding factor 2) gene levels were associated with immune cell infiltration, some checkpoint gene expression, chemotherapy sensitivity, and immunotherapy response. Serum levels of ILF2 were higher in GC patients than in controls, with an AUROC of 0.944 for the diagnosis of GC, and it was also detected in the supernatants of GC cells. Knockdown of ILF2 by siRNA significantly reduced the proliferation and colony formation of GC cells. Overexpression of ILF2 significantly promotes the proliferation and colony formation of gastric cancer cells.

\*Correspondence:  
Kun-He Zhang  
khzhang@ncu.edu.cn

Full list of author information is available at the end of the article



© The Author(s) 2024. **Open Access** This article is licensed under a Creative Commons Attribution 4.0 International License, which permits use, sharing, adaptation, distribution and reproduction in any medium or format, as long as you give appropriate credit to the original author(s) and the source, provide a link to the Creative Commons licence, and indicate if changes were made. The images or other third party material in this article are included in the article's Creative Commons licence, unless indicated otherwise in a credit line to the material. If material is not included in the article's Creative Commons licence and your intended use is not permitted by statutory regulation or exceeds the permitted use, you will need to obtain permission directly from the copyright holder. To view a copy of this licence, visit <http://creativecommons.org/licenses/by/4.0/>. The Creative Commons Public Domain Dedication waiver (<http://creativecommons.org/publicdomain/zero/1.0/>) applies to the data made available in this article, unless otherwise stated in a credit line to the data.

**Conclusions** Trans-omics analysis of proteomics and transcriptomics is an efficient approach for discovering serum biomarkers, and ILF2 is a potential diagnostic biomarker and therapeutic target of gastric cancer.

**Keywords** Gastric cancer, Diagnosis, Serum biomarker, ILF2, Trans-omics analysis, Immune infiltration, Immunotherapy, Chemotherapy

## Introduction

Gastric cancer (GC) is the fifth most common cancer and the fourth leading cause of cancer-related deaths globally, posing a major threat to public health [1]. Many GC patients present with nonspecific symptoms, resulting in diagnosis at an advanced stage and, consequently, an unfavorable prognosis.

GC lacks useful serum biomarkers for clinical diagnosis. Traditional serum biomarkers, such as carcinoembryonic antigen (CEA), carbohydrate antigen 19–9 (CA19-9), carbohydrate antigen 72–4 (CA72-4), and carbohydrate antigen 125 (CA125), provide minimal diagnostic value for GC [2, 3]. Over the past few decades, several circulating biomarkers that indicate the presence of GC have been documented, including gastrin-17 (G-17), pepsinogens (PGs), anti-*Helicobacter pylori* IgG antibodies [4], trefoil factor 3 (TFF3) [5], and metabolic markers such as 3-hydroxypropionic acid [6]. In recent years, this category has been expanded to include circulating tumor cells (CTCs) [7], circulating tumor DNA (ctDNA) [8], and non-coding RNAs (miRNA, lncRNA, and circRNA) [9, 10]. However, the utilization of these biomarkers in clinical settings has been hindered by inadequate diagnostic efficacy and technical complexity. Therefore, it is crucial to discover new serum biomarkers for GC diagnosis.

The combined analysis of proteomics and transcriptomics, a multi-omics approach, holds significant potential in discovering cancer biomarkers [11, 12]. Proteins, as the primary executors of cellular functions, directly reflect changes in cellular states and biological processes, while gene transcription levels offer insights into the potential regulatory mechanisms underlying protein expression. By integrating data from these two layers, researchers can more precisely identify differentially expressed proteins and genes associated with tumorigenesis. This approach facilitates the discovery of novel cancer biomarkers, providing a more solid foundation for early diagnosis, prognostic assessment, and treatment selection [13, 14].

In recent years, cancer immunotherapy has emerged as an innovative and promising approach to cancer treatment and has made remarkable advancements [15]. The integration of bioinformatics analysis with publicly available databases has been particularly effective in identifying potential targets for immunotherapy [16, 17]. The application of multi-omics methods, which combine data from various biological levels, has facilitated the

discovery of novel targets that can significantly improve the survival rates of GC patients. The exploration of immunotherapy targets through bioinformatics and multi-omics approaches holds great promise for improving outcomes in GC and other cancers.

In our previous aptamer-based proteomics study on GC serum, we identified 236 proteins that were differentially expressed in GC serum compared to healthy controls. In the current study, we aimed to further refine this set of proteins and identify those with diagnostic potential for GC. We selected the differentially expressed GC serum proteins that were differentially expressed at the transcriptional level in The Cancer Genome Atlas-Stomach Adenocarcinoma (TCGA-STAD) dataset, followed by lasso regression and random forest analysis to identify key biomarkers. The key biomarkers were independently evaluated for their diagnostic value in GC and bioinformatically analyzed for their associations with various biological behaviors of GC to identify potential serum biomarkers, and the latter were finally validated for their clinical diagnostic value in serum samples and their biological functions in vitro cellular experiments.

## Methods

### Data collection and processing

The differentially expressed serum proteins in our previous aptamer-based GC serum proteomics dataset were identified and their corresponding genes were searched in the UniProt database (<https://www.uniprot.org/>). In the TCGA online database (<https://portal.gdc.cancer.gov/>), mRNA expression data (in transcripts per million) and clinical information were extracted from the STAD dataset (375 tumor tissue samples and 32 normal gastric tissue samples). Differentially expressed genes (DEGs) were identified using the filter criteria of fold change > 1.3 and false discovery rate < 0.05. A cross-analysis between the DEGs in the TCGA-STAD dataset and the genes corresponding to the differentially expressed serum proteins in the GC proteomics dataset was performed to determine overlapping DEGs.

### Trans-omics analysis to identify candidate biomarkers of gastric cancer

Least absolute shrinkage and selection operator (LASSO) regression and random forest (RF) algorithms were used to identify key genes from the overlapping DEGs, and the key genes that overlapped in the results of the two algorithms were designated as candidate biomarkers of GC.

The optimal  $\alpha$  ( $\lambda$ ) value (a parameter that controls feature selection) for LASSO regression was selected by 10-fold cross-validation [18]. For random forest, the decision tree with the lowest out-of-bag (OOB) error rate was selected to evaluate feature importance using the mean decrease gini parameter, and features with the parameter  $>2$  were selected as key genes [19].

#### Internal and external validation

The candidate biomarkers were validated internally using the TCGA-STAD dataset and externally using the Gene Expression Omnibus (GEO) datasets at the mRNA level. Three GEO Series (GSE) datasets were downloaded for external validation: GSE27342 (normal samples: 80; tumor samples: 80), GSE54129 (normal samples: 21; tumor samples: 111), and GSE66229 (normal samples: 100; tumor samples: 300). Batch correction was performed on the three datasets using the “affy” package in the R software. Following dimension reduction through principal component analysis (PCA), a merged GSE dataset containing 201 normal samples and 491 tumor samples was created for external validation.

#### Evaluation of the diagnostic value of candidate biomarkers for GC

The diagnostic performance of the mRNA levels of the potential biomarkers for GC was assessed in both the TCGA-STAD dataset and the merged GSE dataset using the area under the receiver operating characteristic curve (AUROC) as a metric.

#### Potential biomarkers expression and tumor immune infiltration

To examine the differences in immune cell infiltration between the high and low mRNA levels of the potential biomarkers in GC tissues, we employed Cell-type Identification by Estimating Relative Subsets of RNA Transcripts (CIBERSORT) [20]. This tool analyzes immune cell infiltration by assessing gene expression data [21]. We compared the transcriptional levels of genes associated with immune checkpoints between the high and low mRNA level groups of these potential biomarkers [22, 23], including TIGIT (T-cell immunoglobulin and ITIM domain), SIGLEC15 (Sialic acid-binding immunoglobulin-like lectin 15), HAVCR2 (T-cell immunoglobulin and mucin domain-containing protein 3), CD274 (Cluster of Differentiation 274, also known as PD-L1), PDCD1 (Programmed cell death protein 1, also known as PD-1), LAG3 (Lymphocyte-activation gene 3), CTLA4 (Cytotoxic T-lymphocyte-associated antigen 4), and PDCD1LG2 (Programmed cell death 1 ligand 2, also known as PD-L2).

#### Sensitivity to chemotherapy and immunotherapy outcomes based on potential biomarkers expression levels

Data from The Cancer Immunome Atlas (TCIA) database (<https://www.tcia.at/home>) [24, 25] were used to predict the impact of mRNA levels of potential biomarkers on the response to immunotherapy with CTLA4 and PD-1 inhibitors. The Cancer Drug Sensitivity Genomics (GDSC) database ([www.cancerRxgene.org](http://www.cancerRxgene.org)) [26, 27] was used to investigate variations in chemotherapy sensitivity based on high and low mRNA levels of these potential biomarkers.

#### ELISA validation

To confirm the diagnostic significance of potential biomarkers, we obtained serum samples from 30 individuals diagnosed with GC and 22 healthy individuals as controls. Serum levels of ILF2 were measured using a commercially available enzyme-linked immunosorbent assay (ELISA) kit (SAB, USA) according to the manufacturer’s instructions. Briefly, 100  $\mu$ L of serum diluted 1:50 was incubated with capture antibodies at 37 °C for 2 h. After removal of the liquid, 100  $\mu$ L of biotinylated antibody was added and incubated for one hour. After washing three times, streptavidin-HRP conjugate was added and incubated for 1 h. The liquid was then discarded, the wells were washed five times, and tetramethyl benzidine (TMB) substrate was added and incubated for 15 min in the dark. After stopping the reaction, the optical density (OD) values were measured at 450 nm using a JS-THERMO Varioskan Flash (Thermo Fisher Scientific, USA). A standard curve was simultaneously generated and used to determine serum concentrations of the potential biomarkers. The AUROC was used to evaluate the diagnostic value of the potential biomarker.

In addition, the culture supernatants of BGC-823 and GES-1 cells were collected at 24, 48, and 72 h of culture (3000 cells per well) and the levels of potential biomarkers were determined as described above.

#### RT-qPCR

RT-qPCR was utilized to detect the mRNA expression levels of potential biomarkers in the four types of GC cells and the control GES-1 cells. Cells were harvested at their logarithmic growth phase, and total RNA was extracted using a commercial kit provided by Yeasen (China). RNA quantification was performed using NanoDrop 2000 (Thermo Fisher Scientific, USA). Reverse transcription and quantitative PCR amplification of the target genes were performed using Yeasen (China) kits. PCR amplification primers were designed and synthesized by Sangon Biotech Co., Ltd. (Shanghai, China).

### Plasmid extraction

The DH-5 $\alpha$  glycerol bacteria harboring the overexpressed plasmid were provided by Shanghai Genechem Co., Ltd (China). After carefully homogenizing the bacterial suspension, we diluted it by 100, 1000, and 10,000, respectively, and spread the dilutions onto an LB solid culture plates containing ampicillin. The plates were incubated at 37°C for 12–16 h. Following incubation, individual colonies were carefully selected and inoculated into LB liquid medium containing ampicillin. These cultures were incubated with shaking at 37°C and 220 rpm for 12–16 h to amplify bacterial growth. Finally, plasmid extraction was performed using a kit from TIANGEN Biotech(Beijing) Co., Ltd (China).

### Cell culture and transfection

Human gastric cancer cell lines (AGS, MKN45, and HGC27) and normal gastric mucosal epithelial cell line (GES1) were purchased from the Cell Bank of the Chinese Academy of Sciences. The human gastric cancer cell line BGC823 was purchased from Shanghai FuHeng Biology Co., Ltd. (China). These cells were routinely cultured at 37 °C with 5% CO<sub>2</sub>. The cell lines GES-1, HGC27, MKN45, and BGC823 were cultured in RPMI-1640 medium with 10% fetal bovine serum (GIBCO USA), while AGS cells were cultured in DMEM-F12 medium with 10% fetal bovine serum.

To regulate the mRNA expression of potential biomarkers in GC cells, we used small interfering RNA (siRNA) for downregulation and overexpression plasmid for upregulation. GC cells were seeded in cell plates and cultured to 40% confluence. The siRNA sequences and over-expressed plasmids targeting the potential biomarkers were transfected using LIPO3000 reagent (Invitrogen, USA). Following transfection, the cells were incubated for 24–72 h for mRNA level analysis of the potential biomarkers. The siRNA sequences were designed and synthesized by a company (Genepharma, China).

### Cell counting Kit-8

After a 24-hour transfection period, the cells underwent trypsin digestion and were resuspended in a complete culture medium to achieve a concentration of  $2 \times 10^4$  cells/ml. Subsequently, 100  $\mu$ l aliquots of this cell suspension were dispensed into a 96-well plate and incubated under standard cell culture conditions. At specific time intervals (0, 24, 48, 72, and 96 h), 10  $\mu$ l of Cell Counting Kit-8 (CCK-8) reagent (GLPBIO, USA) was added to each well, followed by 2 h of incubation in the dark. Finally, the optical density (OD) was measured at 450 nm using a microplate reader (Thermo Fisher Scientific, USA) and utilized to construct cell proliferation curves.

### Cell clone formation

After a 24-hours transfection period, the cells were detached using trypsin and diluted to achieve a density of 700 cells/ml. Subsequently, 2 ml aliquots of the cell suspension were dispensed into each well of a 6-well plate, and the cultures were maintained with regular medium changes every three days. The incubation period lasted for 14 days or until the majority of individual cell clones exceeded 50 cells. Once the culturing was terminated, the cells were washed with PBS, fixed with 4% paraformaldehyde for 30 min, stained with crystal violet for 10–20 min, and finally rinsed thoroughly with PBS and dried naturally.

### Statistical analysis

The statistical analysis was carried out using R software (version 4.2.2) and GraphPad Prism 8.0 software. Continuous variables are presented as Mean  $\pm$  standard deviation. For comparisons between groups, t-tests were utilized when the data followed a normal distribution. Wilcoxon rank-sum tests were employed for data that did not adhere to a normal distribution.  $P < 0.05$  was statistical significance.

## Results

### Candidate biomarkers identified by trans-omics analysis

In our previous proteomic dataset utilizing aptamers, we identified 236 differentially expressed serum proteins specific to GC (Supplementary Table 1). Their corresponding genes were found in the UniProt database. Analysis of the TCGA-STAD transcriptomic dataset uncovered 10,637 differentially expressed genes (Supplementary Fig. 1). There were 119 overlapping DEGs between the two datasets (Supplementary Table 2, Supplementary Fig. 2).

To identify key DEGs, we employed LASSO regression and random forest analyses on the overlapping DEG set. The LASSO regression with  $\lambda = 0.002$  selected 22 key DEGs (Fig. 1A, B). The random forest analysis pinpointed the 24th decision tree with the lowest OOB error rate of 0.0172 for GC vs. normal sample classification, in which six genes had importance scores  $> 2$ , as evaluated by Gini importance (Fig. 1C, D). The LASSO regression and random forest selection identified four DEGs that overlapped, namely interleukin enhancer-binding factor 2 (ILF2), immunoglobulin J chain (JCHAIN), chromodomain helicase DNA-binding protein 7 (CHD7), and phosphoglucomutase-2-like 1 (PGM2L1) (Fig. 1E), which were designated as candidate biomarkers for GC.

### Validation of candidate biomarker expression

In the TCGA-STAD dataset used for internal validation, ILF2 (Interleukin enhancer-binding factor 2), CHD7 (Chromodomain-helicase-DNA-binding protein 7), and

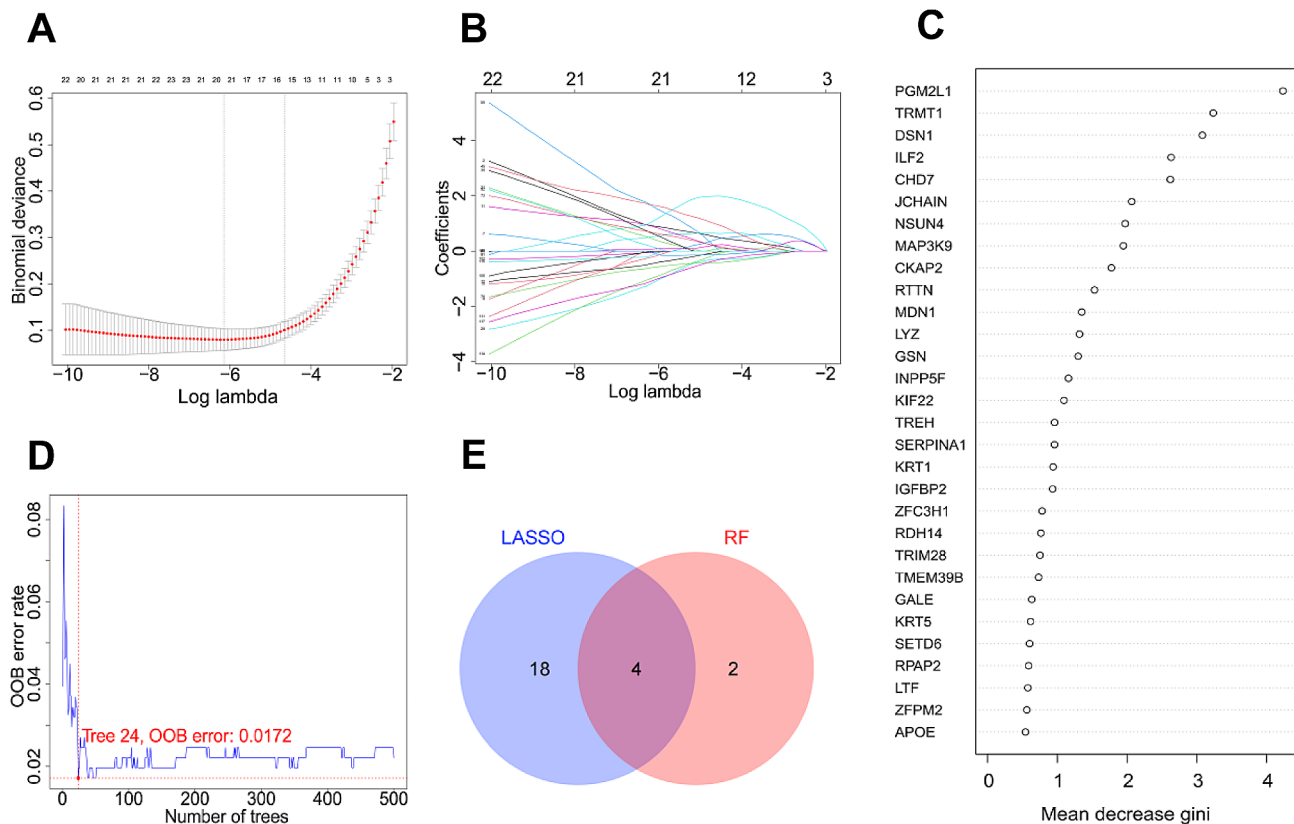


**Fig. 1** Identification of candidate biomarkers for gastric cancer. **A, B:** The selection of key overlapping differentially expressed genes (DEGs) by least absolute shrinkage and selection operator (LASSO) regression analysis. **C, D:** The selection of key overlapping DEGs by random forest (RF) analysis. **E:** Venn diagram of key overlapping DEGs selected by LASSO regression and RF analysis

PGM2L1 (Glucose 1,6-bisphosphate synthase) demonstrated significantly higher mRNA expression levels in GC than in control tissues, whereas JCHAIN (Immunoglobulin J chain) showed significantly lower mRNA expression levels (Fig. 2A). In the external validation using the merged GSE dataset, these candidate biomarkers showed the same trends in mRNA expression levels and significant differences between GC tissues and adjacent normal tissues (Fig. 2B). Before analysis, the external validation datasets (GSE27342, GSE54129, and GSE66229) retrieved from the GEO database underwent standardization, resulting in consistent gene expression distributions (Supplementary Fig. 3A). Following batch-effect correction, the differences among these datasets in the principal component space were significantly reduced (Supplementary Fig. 3B, C), indicating successful merging of the three GES datasets.

#### Diagnostic value of candidate biomarkers for GC

We assessed the diagnostic significance of mRNA levels for the four potential biomarkers in GC using the receiver operating characteristic curve (ROC). In the TCGA-STAD dataset, the AUROCs for diagnosing GC with PGM2L1, ILF2, CHD7, and JCHAIN were

0.950, 0.920, 0.919, and 0.629, respectively (Fig. 2C). In the external validation dataset (the merged GSE dataset), the AUROCs for PGM2L1, ILF2, CHD7, and JCHAIN in diagnosing GC were 0.820, 0.784, 0.745, and 0.736, respectively (Fig. 2D). These results showed that PGM2L1, ILF2, and CHD7 (but not JCHAIN) all had AUROCs greater than 0.7 in both the datasets, highlighting their diagnostic potential for GC and were therefore selected as valuable biomarkers for subsequent studies.

#### Associations of the valuable candidate biomarkers with tumor immunity

Using CIBERSORT analysis, we compared the immune cell infiltration status in GC tissues between high and low expression levels of each biomarker. The results showed that ILF2, CHD7, and PGM2L1 were significantly associated with 14, 11, and 2 of 22 types of infiltrating immune cells, respectively (Fig. 3A–C). From the transcriptome data in the TCGA-STAD dataset, we extracted expression levels of 8 immune checkpoint genes (TIGIT, HAVCR2, CD274, SIGLEC15, LAG3, PDCD1, PDCD1LG2, and CTLA4). Comparing differences in their expression between high and low levels of each biomarker, we found that ILF2 expression was significantly associated with

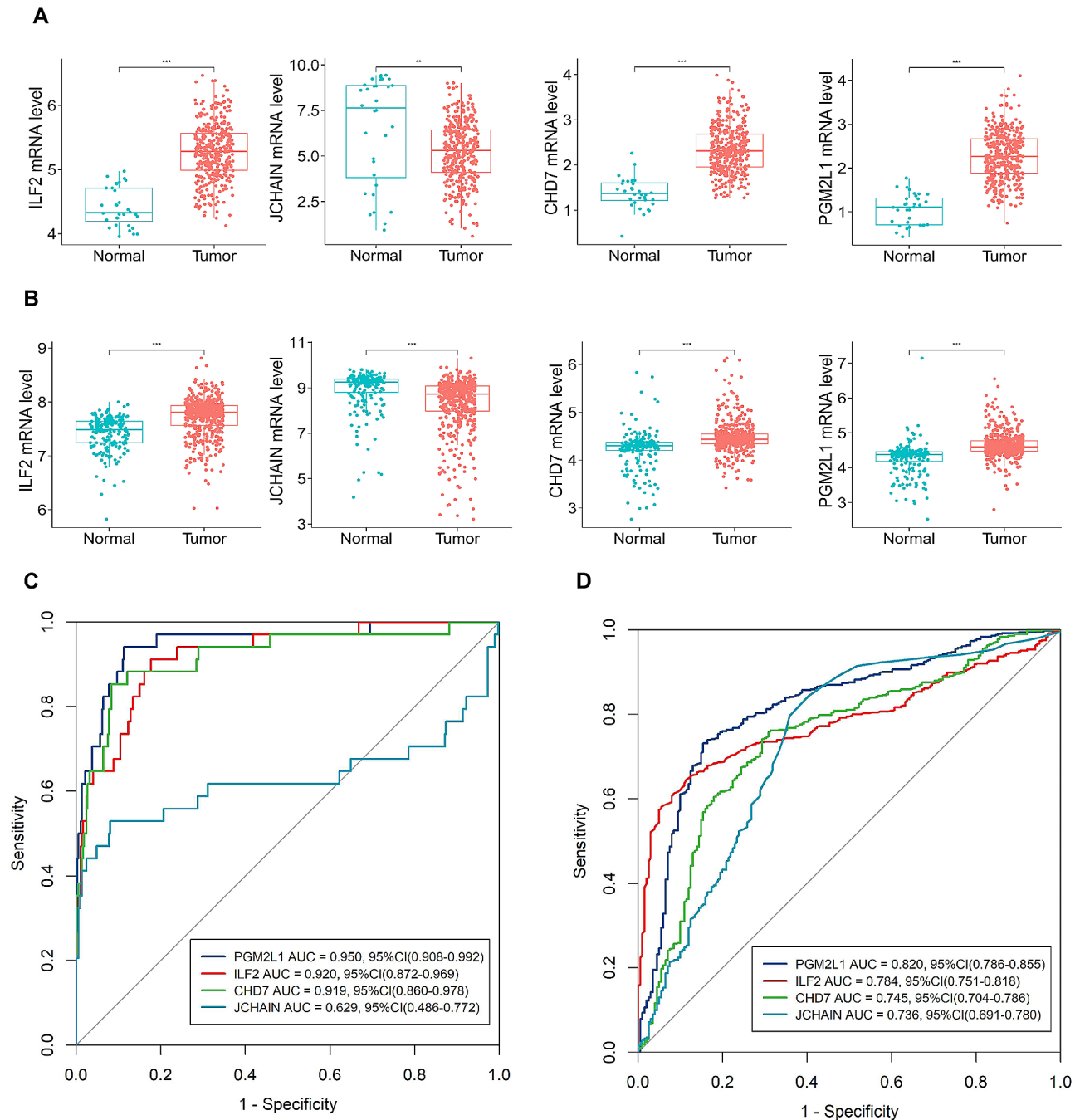


**Fig. 2** Expression and diagnosis value of the four candidate biomarkers in gastric cancer and normal control tissues. \*  $P < 0.05$ , \*\*  $P < 0.01$ , \*\*\*  $P < 0.001$ . **A:** STAD dataset from The Cancer Genome Atlas database; **B:** Merged datasets of GSE27342, GSE54129 and GSE66229 datasets from the Gene Expression Omnibus (GEO) database. **C:** STAD dataset from The Cancer Genome Atlas database; **D:** Merged dataset of GSE27342, GSE54129 and GSE66229 datasets from the Gene Expression Omnibus (GEO) database; AUC: area under the curve

CD274, CTLA4, and SIGLEC15; CHD7 was significantly associated with CD274; and PGM2L1 was significantly associated with SIGLEC15 (Fig. 4A-C). These findings suggest that, among the three biomarkers, ILF2 exhibits the strongest association with tumor immunity in GC, involving multiple immune checkpoint genes. Therefore,

ILF2 was selected as a potential biomarker for subsequent studies.

#### Associations of ILF2 with immunotherapy and chemotherapy responses

We utilized the GDSC database to analyze the variations in response to standard chemotherapy drugs

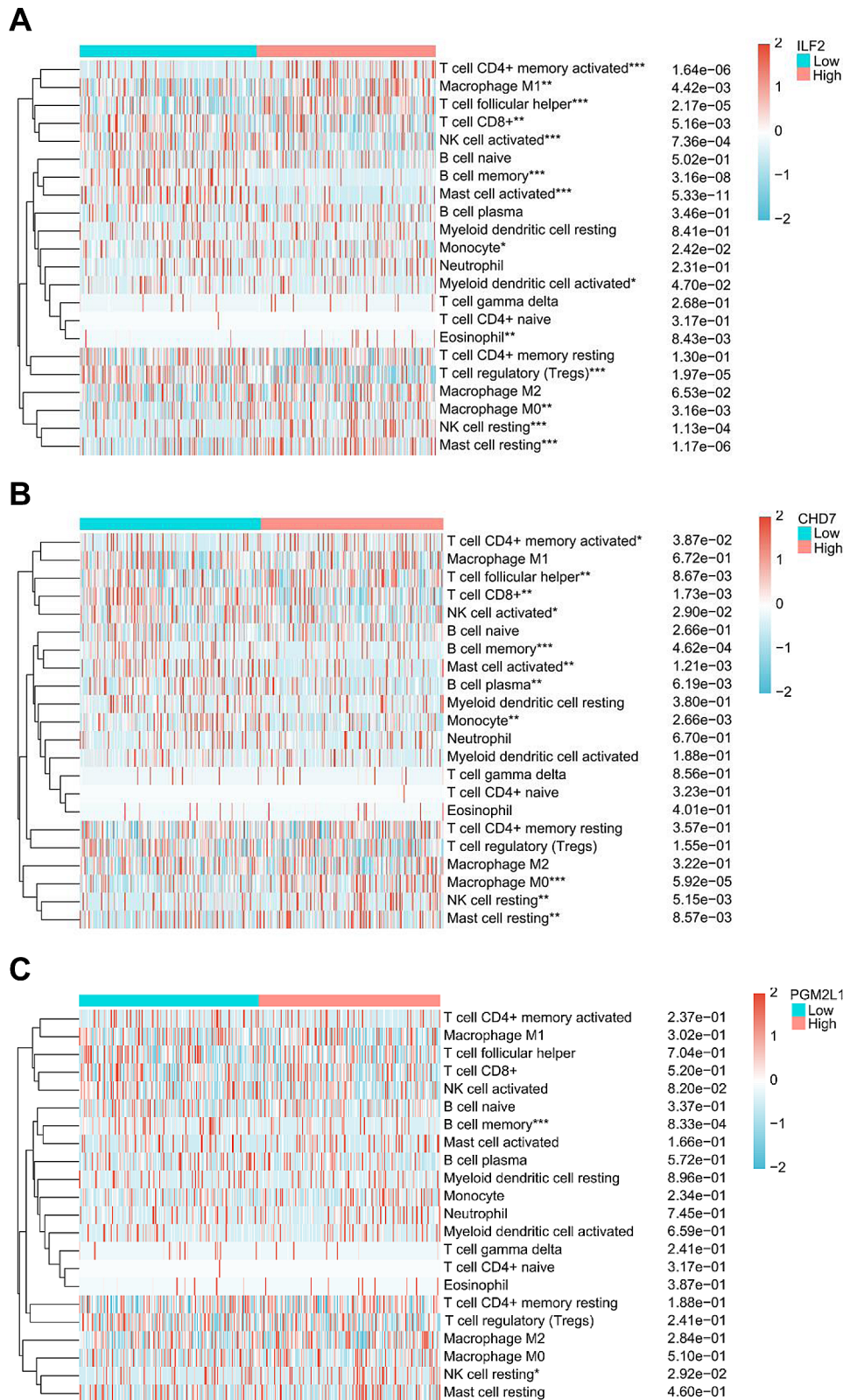


**Fig. 3** Heatmaps of immune cell scores and comparisons between high and low biomarker expression groups. \* $P < 0.05$ , \*\* $P < 0.01$ , \*\*\* $P < 0.001$ . **A:** ILF2; **B:** CHD7; **C:** PGM2L1

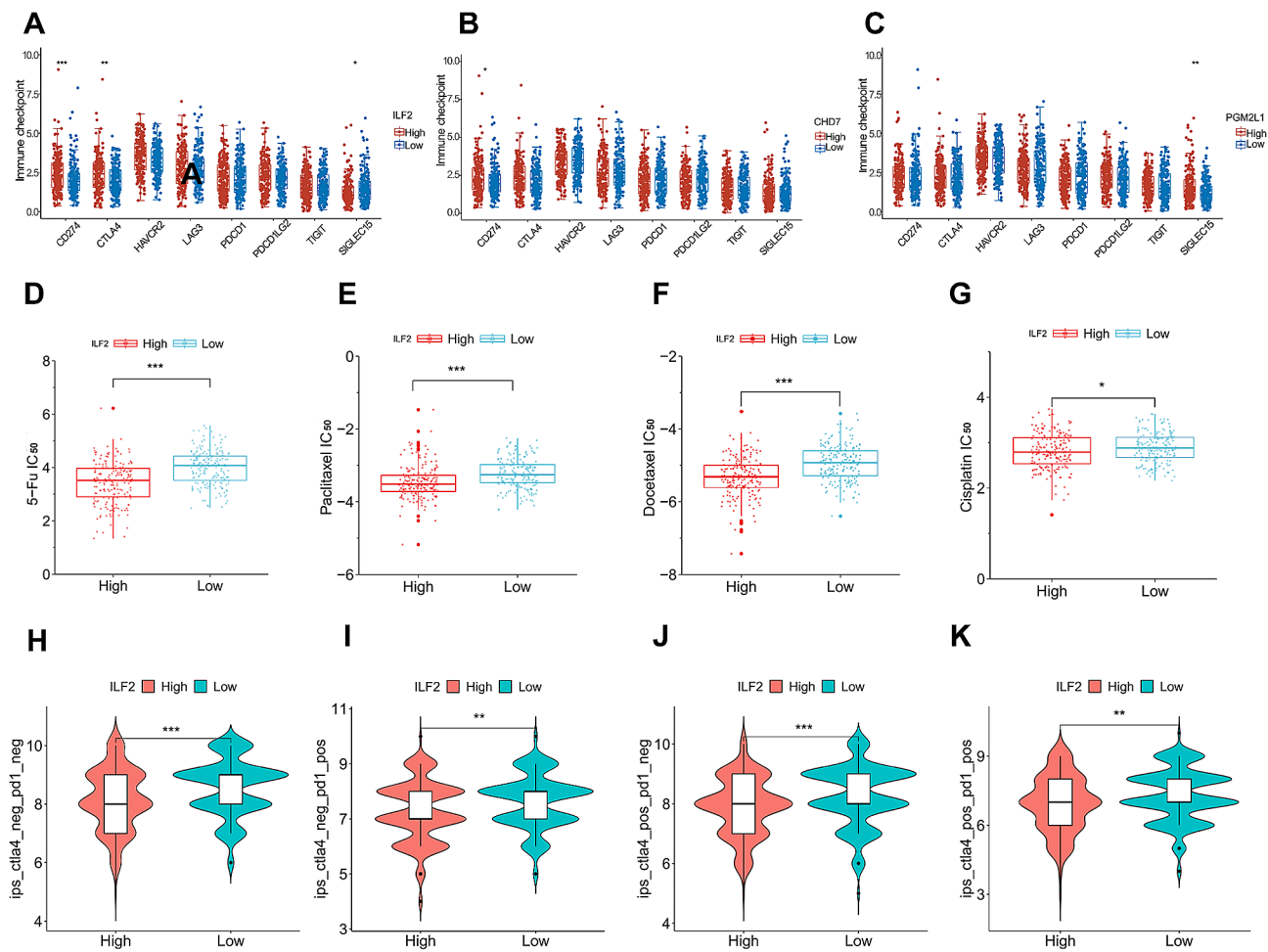


**Fig. 4** Bioinformatics analyses of ILF2 in gastric cancer. \* $P < 0.05$ , \*\* $P < 0.01$ , \*\*\* $P < 0.001$ . **A-C**: Comparison of immune checkpoint-related gene expression levels between the high and low expression groups of biomarkers. **D-G**: Comparison of sensitivity to anticancer drugs between the high and low ILF2 expression groups. **H-K**: Comparison of response to immunotherapy between the high and low ILF2 expression groups; IPS, the Immunophenoscore; POS, positive; NEG, negative

(5-fluorouracil, paclitaxel, docetaxel, and cisplatin) [26] among gastric cancer patients with different levels of ILF2 expression. The findings indicate that the IC<sub>50</sub>s were lower in the high-level ILF2 group compared with the low-level ILF2 group. Hence, GC with increased ILF2 levels exhibits enhanced response to these drugs (Fig. 4D-G). Additionally, using the TCIA database, we calculated CTLA4- and PD-1-based immunophenotype scores (IPS) for GC patients and compared the response to anti-CTLA4 and anti-PD-1 immunotherapy between patients with high and low ILF2 expression levels. The results indicated that individuals with elevated ILF2 levels exhibited significantly attenuated responses to CTLA4 and PD-1 inhibitors (Fig. 4H-K).

#### Clinical validation of the diagnostic significance of serum ILF2 levels in gastric cancer

Utilizing ELISA (its standard curve shown in Figure 5A), serum levels of ILF2 protein were measured and notably

elevated in the GC group when compared to the control group ( $443.23 \pm 303.29$  ng/mL vs.  $72.31 \pm 45.18$  ng/mL,  $P < 0.0001$ ) (Fig. 5, B). ILF2 levels were valuable for diagnosing GC with an AUROC of 0.944 (Fig. 5C). The baseline information of the patients is shown in Supplementary Table S3.

#### Detection of ILF2 expression in the supernatant of gastric cancer cell culture

The presence of ILF2 protein was observed in the culture supernatants of BGC823 GC cells, and its concentration increased as the culture time progressed. However, it was not detected in the supernatants of GES-1 gastric epithelial cells (Fig. 5D), indicating that gastric cancer cells can secrete ILF2.

#### Expression levels of ILF2 in GC cells

The ILF2 mRNA expression was detected by RT-qPCR in four GC cell lines (AGS, MKN45, HGC27, and BGC823)



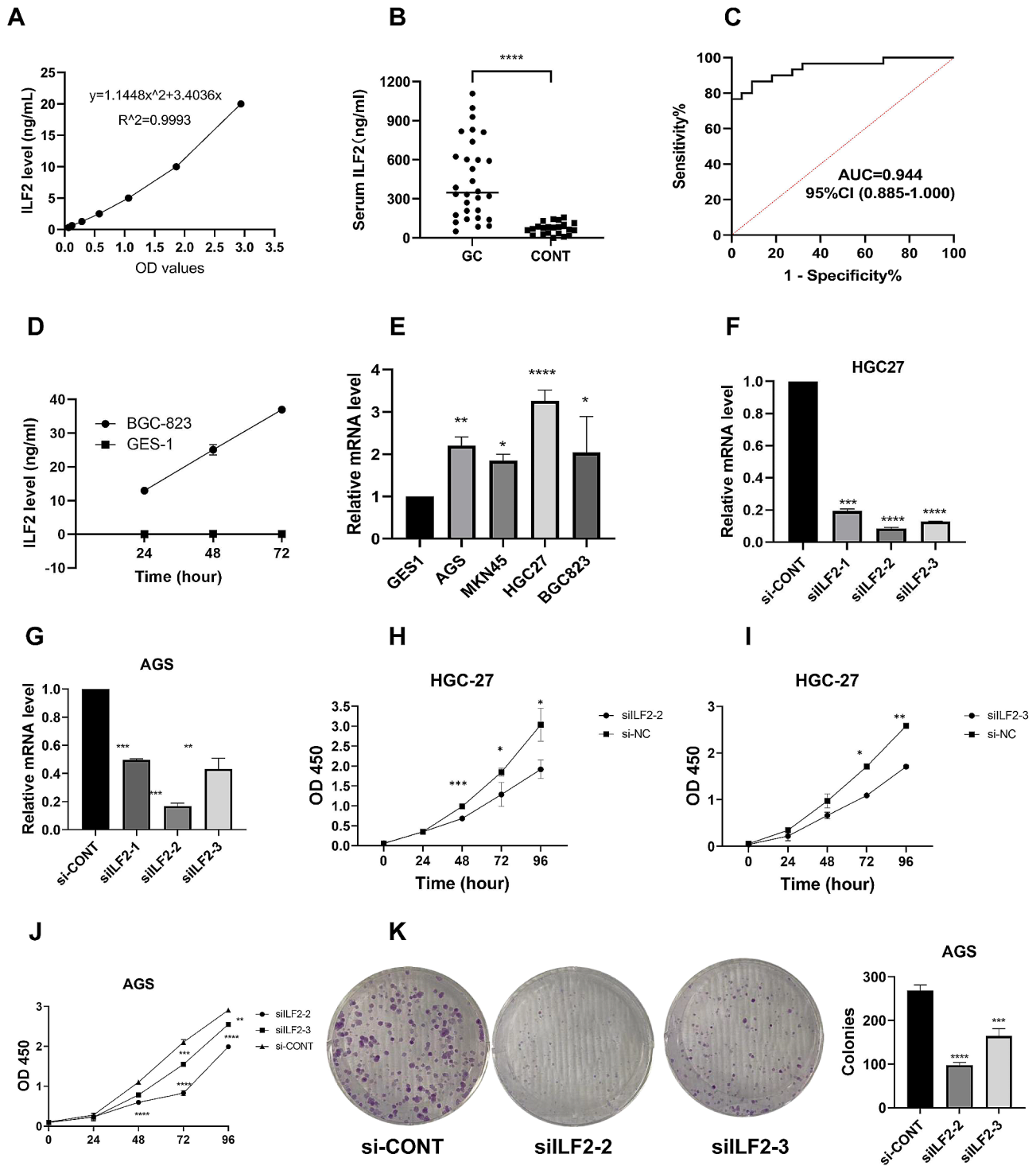


**Fig. 5** Clinical and functional validation of ILF2. **A:** The standard curve for the detection of ILF2 by enzyme-linked immunosorbent assay. **B:** Serum ILF2 levels and comparison between gastric cancer and control group. **C:** The receiver operating characteristic curve of serum ILF2 levels for the diagnosis of gastric cancer. **D:** ILF2 levels in cell culture supernatants. **E:** Relative mRNA expression levels of ILF2 in different gastric cancer cell lines; **F, G:** The effect of siRNA-mediated ILF2 knockdown on mRNA expression in HGC-27 and AGS cells; **H-J:** Comparisons of HGC-27 cell proliferation between siRNA-mediated ILF2 knockdown and control groups. **K:** The effect of siRNA-mediated ILF2 knockdown on clone formation in AGS cells. AUC, Area Under Curve; CI, Confidence Interval; OD, Optical Density

and one control cell line (GES-1). The primer sequences used for the PCR amplification of ILF2 were 5'-GGGGAACAAAGTCGTGGAAAG-3' (forward) and 5'-CCAGTTTCGTTGGTCAGCA-3' (reverse). The results indicated a significant upregulation of ILF2 mRNA expression in all four GC cell lines compared to the control (Fig. 5E).

#### Effect of ILF2 knockdown on GC cell growth

We knocked down ILF2 transcription using siRNAs in HGC27 and AGS cells. Three ILF2 mRNA-specific siRNA sequences (siILF2-1, siILF2-2, and siILF2-3) and one control sequence (siILF2-CONT) were employed in the knockdown experiments. Their nucleic acid sequences (sense) were as follows:

siILF2-1: 5'-GAUAGUAACACCUUCAGAATT-3'

siILF2-2: 5'-CUUUGUACCACAUUCCCAT-3'

siILF2-3: 5'-GCUACAGUGAAGAUUCUCATT-3'

siILF2-CONT: 5'-UUUCUCCGAACGUGUCACGUT-3'

The findings indicated that the siRNA depletion notably reduced the ILF2 mRNA levels (Fig. 5F, G). Among the three siRNAs, siILF2-2 exhibited the most effective knockdown. In CCK-8 experiments, there was a notable reduction in cell proliferation at 48, 72, and 96 h in HGC27 cells and 72 and 96 h in AGS cells transfected with siILF2-2 and siILF2-3 compared to the control (Fig. 5H-J). In clone formation experiments (Fig. 5K), the number of AGS cell clones with knocked-down ILF2 decreased significantly.

#### Effect of ILF2 overexpression on the growth of gastric cancer cells

The ILF2 overexpression plasmid was designed by Shanghai Genechem Co., Ltd (China), and vector details are presented in Fig. 6A. The results indicated that ILF2 overexpression significantly increased the level of ILF2 mRNA, as demonstrated in Fig. 6B, C. In the CCK-8 assay, BGC823 and MKN45 cells with overexpression of ILF2 exhibited significantly enhanced proliferative capacity compared to the control group (Fig. 6D-E). Additionally, in the clone formation experiment (Fig. 6F), the number of MKN45 cell clones overexpressing ILF2 increased significantly.

#### Discussion

Through the cross-analysis of our aptamer-based serum proteomic dataset and the TCGA-STAD tissue transcriptomic dataset, we have discovered four candidate biomarkers for GC: ILF2, JCHAIN, PGM2L1, and CHD7. Except for JCHAIN, all the candidate biomarkers proved useful in diagnosing GC in both the TCGA-STAD and the merged GSE dataset. Among the three candidate biomarkers with significant value, ILF2 stood out as it exhibited a strong correlation with the infiltration of immune

cells and the expression of immune checkpoint genes in GC. As a result, ILF2 was selected as a promising diagnostic biomarker for GC. Subsequent studies showed that ILF2 was significantly associated with GC in terms of chemotherapy sensitivity and immunotherapy response. In the clinical validation study, ILF2 protein levels were significantly elevated in GC serum samples and exhibited good diagnostic performance for GC. In vitro experiments demonstrated that GC cells exhibited elevated levels of ILF2 expression and the ability to secrete ILF2. The suppression of ILF2 expression impeded the proliferation and clone formation of GC cells, while overexpression of ILF2 promoted these processes.

ILF2, also known as nuclear factor 45 (NF45), interacts with different partners to play a role in controlling gene expression at both the transcriptional and post-transcriptional stages. By binding to the interleukin-2 enhancer, ILF2 promotes the transcription of interleukin-2 in activated T cells [28]. ILF2 can interact with lncRNA, a type of ribonucleic acid that does not code for proteins, to control the maturation of miRNA [29]. Additionally, ILF2 can also interact with nuclear proteins like YB-1 to regulate the processes of RNA splicing and degradation [30].

ILF2 gene amplification and overexpression in different human cancers promote cellular processes such as cell growth, programmed cell death, and invasion [31]. ILF2 is upregulated in several malignancies, including liver and lung cancer, where its high expression stimulates malignant phenotypes in liver cells [32, 33] and interacts with E2F transcription factor 1 (E2F1) to promote lung cancer progression [34]. The suppression of ILF2 expression leads to improved prognosis in breast cancer [35].

Reports on the study of ILF2 in GC are limited. Yin et al. [36] first detected the ILF2 expression levels in both tumor and paired normal tissues of GC using qRT-PCR, Western blot, and immunohistochemistry, and found that ILF2 was predominantly localized to the nuclei of gastric cancer cells, and also exhibited a low level of expression in the cytoplasm. Furthermore, the overexpression of ILF2 in tumor tissues had substantial prognostic significance in gastric cancer. Arai et al. [37] further identified ILF2 as a notable protein present in both gastric cancer tissues and cell lines, functioning as a DNA damage response (DDR) protein. In addition, the ILF2/ILF3 complex dynamically regulates the expression of lncRNA ELF3-AS1 and transcription factor ELF3, thereby influencing GC metastasis [38]. However, the impact of ILF2 on GC diagnosis and therapy and the association of ILF2 with GC cell growth and tumor immunity remain unclear.

In the present study, we found that ILF2 had a good diagnostic value for GC. The high expression of ILF2 at the transcriptional level in GC tissues effectively distinguished cancer tissues from control tissues, which was

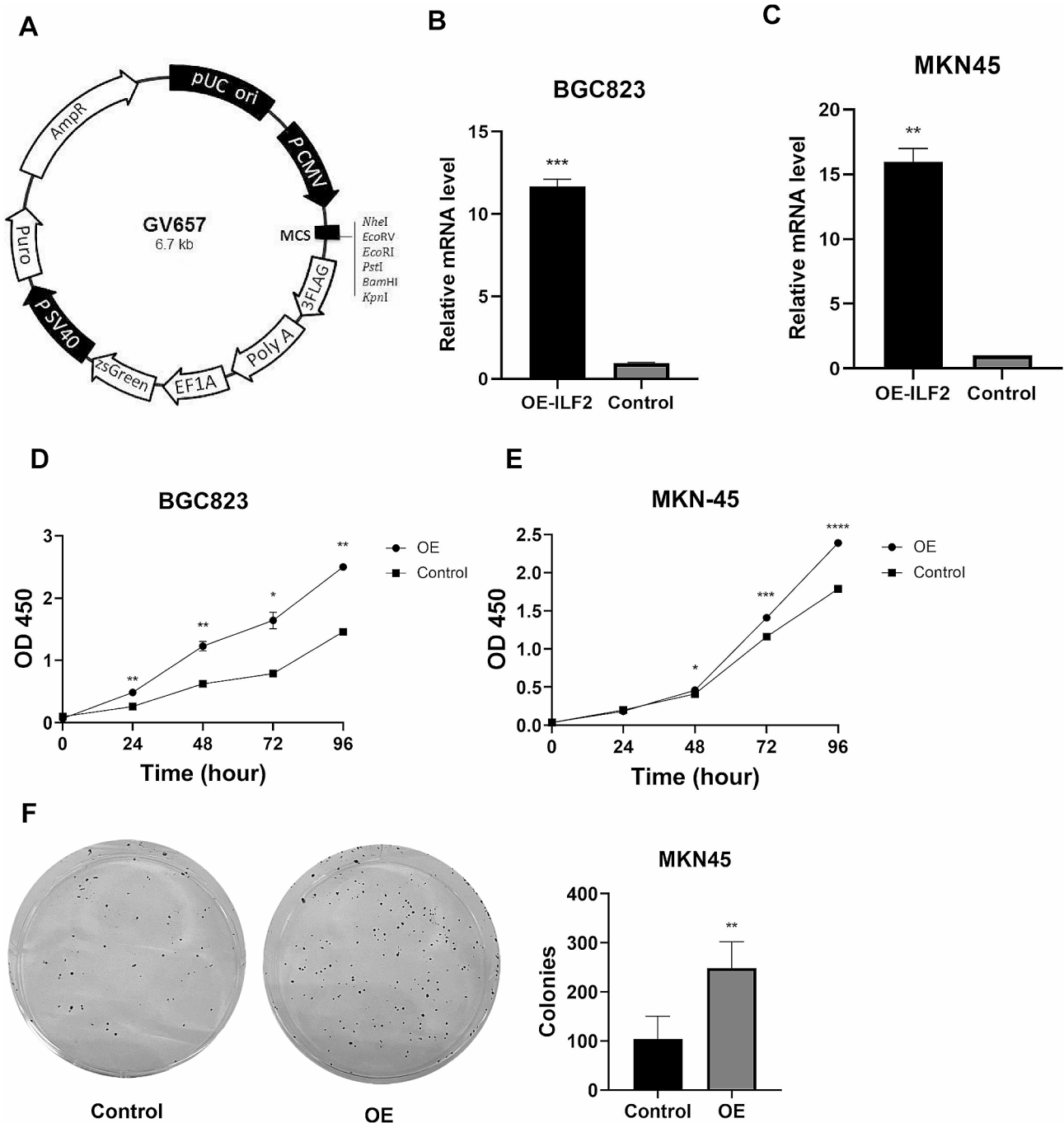


**Fig. 6** The effect of overexpressing ILF2 on the function of gastric cancer cells. **A** The vector of ILF2. **B, C** The effect of ILF2 overexpression on mRNA expression in BGC823 and MKN45 cells. **D, E**: Comparisons of cell proliferation between ILF2 over-expressed groups and control groups in BGC823 and MKN45 cells. **F**. The effect of ILF2 over-expressed on clone formation in MKN45 cells. OE, over expression

confirmed not only in the discovery dataset (TCGA-STAD dataset) but also in the large-sample validation dataset merged from three independent GSE datasets of GC. More importantly, we also detected an elevated level of ILF2 in the serum samples of GC patients, approximately 6-fold higher than that of control samples. The AUROC for the diagnosis of GC reached 0.944. Given the

absence of a valuable serum biomarker for GC and the ease of collecting serum samples in clinical practice, our discovery suggests a promising opportunity for clinical application and warrants additional investigation.

The findings of this research offer a solid biological foundation for the considerable diagnostic importance of ILF2 in GC. Through bioinformatics analysis, we

discovered a strong correlation between ILF2 expression levels in GC tissues and tumor immunity, encompassing immune cell infiltration, expression of immune checkpoint genes, immunotherapy response, as well as chemosensitivity. In vitro experiments demonstrated that GC cell lines overexpressing ILF2 secreted the protein extracellularly and exhibited different chemosensitivity based on ILF2 expression levels. Moreover, the knock-down of ILF2 expression inhibited cell proliferation and colony formation, and overexpression of ILF2 promoted the proliferation and colony formation of gastric cancer cells. However, the question here is how ILF2, a nuclear protein, is secreted outside the cell. Future studies are required to clarify the unclear underlying mechanism.

In this study, we used multiple datasets, including the TCGA-STAD dataset, the GEO dataset, and our serum proteomics dataset and serum specimen dataset. The good representation of datasets from different sources used in the same study favors obtaining research results with better generalization. However, some limitations of these datasets may cause bias; for example, the TCGA-STAD dataset has an imbalance in case numbers between gastric cancer and control groups, there are differences in RNA-Seq data between the GEO datasets (although compensated by data processing techniques), and our own serum sample dataset has a small sample size and insufficient control groups. Although we have successfully screened and validated ILF2 as a valuable biomarker for gastric cancer through rigorous multistep screening and validation, a larger sample size and multicenter validation of the results are still needed.

Moreover, further elucidation is needed in several areas, including clarifying the mechanism by which gastric cancer cells secrete ILF2 and investigating the impact of inhibiting the functional activity of extracellular ILF2 with neutralizing antibodies or small molecules (if available) on the biological behavior of gastric cancer, which will be crucial for revealing the therapeutic potential of ILF2. Additionally, in-depth research is required to understand how ILF2 regulates the biological behaviors of gastric cancer and assess the influence of ILF2 expression on migration, invasion phenotypes, and immune modulation in gastric cancer. To gain a deeper understanding of the role and exact regulatory mechanisms of ILF2 in gastric cancer, further in vivo and in vitro studies are essential.

## Conclusions

In this study, we utilized cross-omics analysis and identified ILF2 as a promising serum diagnostic marker for gastric cancer, exhibiting good diagnostic value and applicability. Bioinformatics analysis revealed a significant correlation between ILF2 and immune status and therapeutic response in gastric cancer. In vitro

experiments confirmed that ILF2 is highly expressed in gastric cancer cells and influences cell growth. ILF2 levels were significantly elevated in the serum of gastric cancer patients, demonstrating its diagnostic significance. However, there are still several related issues that require clarification, including the secretion mechanism of ILF2 from gastric cancer cells and the precise mechanism by which ILF2 regulates the biological behaviors of gastric cancer. Furthermore, the diagnostic significance of serum ILF2 concentration for gastric cancer should be validated through large-sample and multicenter studies.

## Abbreviations

5-FU	5-Fluorouracil
AUROC	Receiver operating characteristic curve
CA125	Carbohydrate antigen 125
CA19-9	Carbohydrate antigen 19–9
CA72-4	Carbohydrate antigen 72–4
CCK-8	Cell Counting Kit-8
CEA	Carcinoembryonic antigen
CHD7	Chromodomain helicase DNA-binding protein 7
CIBERSORT	Cell-type Identification by Estimating Relative Subsets of RNA Transcripts
CTCs	Circulating tumor cells
ctDNA	Circulating tumor DNA
CTLA4	Cytotoxic T-lymphocyte-associated antigen 4
DEGs	Differentially expressed genes
ELISA	Enzyme-linked immunosorbent assay
G-17	Gastrin-17
GC	Gastric cancer
GDSC	The Cancer Drug Sensitivity Genomics
GEO	Gene Expression Omnibus
ILF2	Interleukin enhancer-binding factor 2
JCHAIN	Immunoglobulin J chain
OD	Optical density
OOB	Out-of-bag
PD-1	Programmed cell death protein-1
PGM2L1	Phosphoglucomutase-2-like 1
PGs	Pepsinogens
siRNA	Small interfering RNA
TCGA-STAD	The Cancer Genome Atlas-Stomach Adenocarcinoma
TCGA	The Cancer Genome Atlas
TCIA	The Cancer Immunome Atlas
TFF3	Trefoil factor 3
TMB	Tetra methyl benzidine

## Supplementary Information

The online version contains supplementary material available at <https://doi.org/10.1186/s12885-024-12175-z>.

Supplementary Material 1

## Acknowledgements

Not applicable.

## Author contributions

All authors contributed to the study conception and design. Material preparation, data collection and analysis were performed by Qin-Si Wan, Cong Lv, Jin-Ke Wang, Song Jiang, Dan Cai, and Mao-Sheng Liu. The first draft of the manuscript was written by Shao-Song Liu. Ting Wang and Kun-He Zhang revised the manuscript and all authors commented on previous versions of the manuscript. All authors read and approved the final manuscript.

**Funding**

This work was supported by the National Natural Science Foundation of China (82160494).

**Data availability**

The datasets used and/or analysed during the current study are available from the corresponding author on reasonable request.

**Declarations****Ethics approval and consent to participate**

This research was approved by the Ethics Committee of The First Affiliated Hospital of Nanchang University. All examinations in humans were conducted according to the Declaration of Helsinki and its amendments. All procedures performed in studies involving human participants were approved by the Ethics Committee of The First Affiliated Hospital of Nanchang University. All methods were carried out in accordance with relevant guidelines and regulations. The Ethics Committee of the First Affiliated Hospital of Nanchang University waived the requirement for patient informed consent because the assay for ILF2 used previously collected frozen leftover serum specimens from biochemical assays, not specifically drawn blood specimens.

**Consent for publication**

Not applicable.

**Competing interests**

The authors declare no competing interests.

**Author details**

<sup>1</sup>Department of Gastroenterology, The First Affiliated Hospital, Jiangxi Medical College, Nanchang University; Jiangxi Institute of Gastroenterology & Hepatology, Nanchang, China, No 17, Yongwai Zheng Street, 330006 Nanchang, China

Received: 26 January 2024 / Accepted: 24 March 2024

Published online: 15 April 2024

**References**

- Sung H, et al. Global cancer statistics 2020: GLOBOCAN estimates of incidence and mortality worldwide for 36 cancers in 185 countries. *CA Cancer J Clin*. 2021;71(3):209–49.
- Matsuoka T, Yashiro M. Biomarkers of gastric cancer: current topics and future perspective. *World J Gastroenterol*. 2018;24(26):2818–32.
- Feng F, et al. Diagnostic and prognostic value of CEA, CA19-9, AFP and CA125 for early gastric cancer. *BMC Cancer*. 2017;17(1):737.
- Cai Q, et al. Development and validation of a prediction rule for estimating gastric cancer risk in the Chinese high-risk population: a nationwide multi-centre study. *Gut*. 2019;68(9):1576–87.
- Kaise M, et al. The combination of serum trefoil factor 3 and pepsinogen testing is a valid non-endoscopic biomarker for predicting the presence of gastric cancer: a new marker for gastric cancer risk. *J Gastroenterol*. 2011;46(6):736–45.
- Ikeda A, et al. Serum metabolomics as a novel diagnostic approach for gastrointestinal cancer. *Biomed Chromatogr*. 2012;26(5):548–58.
- Thanh HP, et al. Emerging role of circulating tumor cells in gastric cancer. *Cancers (Basel)*. 2020;12(3).
- Zhang Z, et al. Liquid biopsy in gastric cancer: predictive and prognostic biomarkers. *Cell Death Dis*. 2022;13(10):903.
- Yuan L, et al. Long non-coding RNAs towards precision medicine in gastric cancer: early diagnosis, treatment, and drug resistance. *Mol Cancer*. 2020;19(1):96.
- Shan C, et al. Biogenesis, functions and clinical significance of circRNAs in gastric cancer. *Mol Cancer*. 2019;18(1):136.
- Wang K, Huang C, Nice EC. Proteomics, genomics and transcriptomics: their emerging roles in the discovery and validation of colorectal cancer biomarkers. *Expert Rev Proteom*. 2014;11(2):179–205.
- Yang W, et al. Integrating proteomics and transcriptomics for the identification of potential targets in early colorectal cancer. *Int J Oncol*. 2019;55(2):439–50.
- Bartha Á, et al. Proteotranscriptomic discrimination of tumor and normal tissues in renal cell carcinoma. *Int J Mol Sci*. 2023;24(5).
- Lapitz A, et al. Liquid biopsy-based protein biomarkers for risk prediction, early diagnosis, and prognostication of cholangiocarcinoma. *J Hepatol*. 2023;79(1):93–108.
- Hirsch FR, et al. Lung cancer: current therapies and new targeted treatments. *Lancet*. 2017;389(10066):299–311.
- Blum A, Wang P, Zenklusen JC. Snapshot: TCGA-analyzed tumors. *Cell*. 2018;173(2):530.
- Ucaryilmaz MC, Ozcan G. Comprehensive bioinformatic analysis reveals a cancer-associated fibroblast gene signature as a poor prognostic factor and potential therapeutic target in gastric cancer. *BMC Cancer*. 2022;22(1):692.
- Wang Q, et al. Nomogram established on account of Lasso-Cox regression for predicting recurrence in patients with early-stage hepatocellular carcinoma. *Front Immunol*. 2022;13:1019638.
- Chen W, et al. Screening diagnostic markers for acute myeloid leukemia based on bioinformatics analysis. *Transl Cancer Res*. 2022;11(6):1722–9.
- Newman AM, et al. Robust enumeration of cell subsets from tissue expression profiles. *Nat Methods*. 2015;12(5):453–7.
- Zeng D, et al. Gene expression profiles for a prognostic immunoscore in gastric cancer. *Br J Surg*. 2018;105(10):1338–48.
- Wang J, et al. Siglec-15 as an immune suppressor and potential target for normalization cancer immunotherapy. *Nat Med*. 2019;25(4):656–66.
- Zeng D, et al. Tumor microenvironment characterization in gastric cancer identifies prognostic and immunotherapeutically relevant gene signatures. *Cancer Immunol Res*. 2019;7(5):737–50.
- Van Allen EM, et al. Genomic correlates of response to CTLA-4 blockade in metastatic melanoma. *Science*. 2015;350(6257):207–11.
- Hugo W, et al. Genomic and transcriptomic features of response to anti-PD-1 therapy in metastatic melanoma. *Cell*. 2016;165(1):35–44.
- Iorio F, et al. A landscape of pharmacogenomic interactions in cancer. *Cell*. 2016;166(3):740–54.
- Yang W, et al. Genomics of drug sensitivity in cancer (GDSC): a resource for therapeutic biomarker discovery in cancer cells. *Nucleic Acids Res*. 2013;41(Database issue):D955–61.
- Kao PN, et al. Cloning and expression of cyclosporin A- and FK506-sensitive nuclear factor of activated T-cells: NF45 and NF90. *J Biol Chem*. 1994;269(32):20691–9.
- Zhang Y, et al. lncRNA AK085865 promotes macrophage M2 polarization in CVB3-induced VM by regulating ILF2-ILF3 complex-mediated miRNA-192 biogenesis. *Mol Ther Nucleic Acids*. 2020;21:441–51.
- Marchesini M, et al. ILF2 is a regulator of RNA splicing and DNA damage response in 1q21-amplified multiple myeloma. *Cancer Cell*. 2017;32(1):88–e1006.
- Zhang X, et al. Interleukin enhancer-binding factor 2 promotes cell proliferation and DNA damage response in metastatic melanoma. *Clin Transl Med*. 2021;11(10):e608.
- Du H, et al. ILF2 directly binds and stabilizes CREB to stimulate malignant phenotypes of liver cancer cells. *Anal Cell Pathol (Amst)*. 2019;2019:1575031.
- Cheng S, et al. Expression and critical role of interleukin enhancer binding factor 2 in Hepatocellular Carcinoma. *Int J Mol Sci*. 2016;17(8).
- Zhao M, et al. ILF2 cooperates with E2F1 to maintain mitochondrial homeostasis and promote small cell lung cancer progression. *Cancer Biol Med*. 2019;16(4):771–83.
- Noblejas-López M, et al. Genomic mapping of splicing-related genes identify amplifications in LSM1, CLNS1A, and ILF2 in luminal breast cancer. *Cancers (Basel)*. 2021;13(16).
- Yin ZH, et al. Expression and clinical significance of ILF2 in gastric cancer. *Dis Markers*. 2017;2017:4387081.
- Arai H, et al. Expression of DNA damage response proteins in gastric cancer: comprehensive protein profiling and histological analysis. *Int J Oncol*. 2018;52(3):978–88.
- Li D, et al. lncRNA ELF3-AS1 inhibits gastric cancer by forming a negative feedback loop with SNAI2 and regulates ELF3 mRNA stability via interacting with ILF2/ILF3 complex. *J Exp Clin Cancer Res*. 2022;41(1):332.

**Publisher's Note**

Springer Nature remains neutral with regard to jurisdictional claims in published maps and institutional affiliations.